

# A Nonthermal Chemicurrent Effect of Hydrogen Adsorption on Pt/SiC Planar Nanostructures at Normal Ambient Conditions

S. K. Dasari<sup>a</sup>, M. A. Hashemian<sup>a</sup>, J. Mohan<sup>a</sup>, E. G. Karpov<sup>a,\*</sup>

<sup>a</sup>*Department of Civil and Materials Engineering, University of Illinois at Chicago,  
Chicago, IL 60607, USA*

---

## Abstract

Reaction induced currents in planar metal/semiconductor nanostructures can provide a direct insight into underlying charge transfer processes involved in chemical energy dissipation at solid surfaces. This letter provides clear evidence of the non-thermal nature of chemicurrent induced by H<sub>2</sub> adsorption on a Pt/SiC nanostructure at room temperature in 760 Torr N<sub>2</sub>/O<sub>2</sub> mixtures with various oxygen fractions. The thermal effect of the reaction is reproduced also with admission of N<sub>2</sub> molecules to the sample. Only the process with H<sub>2</sub> leads to a detectable chemicurrent proving participation of nonthermal electrons in the charge transfer induced by hydrogen evolution on the nanostructure surface.

---

\* Corresponding author; email: ekarpov@uic.edu

## 1 Introduction

Understanding of the basic charge transfer processes at solid interfaces with reactive gas mixtures is a pathway toward advanced sensing, novel catalysts and energy conversion applications. In particular, currents induced in surface reactions on catalytic nanofilms forming a Schottky or metal-oxide-semiconductor (MOS) type contact with a semiconductor substrate have received considerable attention during the last decade [1–18]. The physical nature of these currents is intriguing, because such a nanofilm device contains no explicit ion conductive layers and it resembles a photovoltaic cell much more closely than an electrochemical device. For this reason, chemically induced currents in material systems governed by only electronic conductance are often called "chemicurrents" by analogy with photocurrents. Several groups of authors [1–16] describe the chemicurrents from the standpoint of nonadiabatic surface chemistry [8,9,20–24] similar to one responsible for heterogenous chemiluminescence [20,25,26], and related phenomena [27–30]. Here, the surface released chemical energy is transferred directly to the electron subsystem of the solid catalyst to produce a population of mobile hot electrons in the metal nanofilm or e-h pairs in a semiconductor layer able to travel over the internal potential barrier, which performs a charge separation function, Figure 1. Such currents, therefore, could directly represent basic mechanisms of charge transfer in chemical transformations on solid surfaces, and their nonadiabatic origin in adsorption related process at cryogenic temperatures and vacuum conditions [7–12] is well recognized. Chemicurrents generated in the course of continuous catalytic oxidation of molecular hydrogen [4,5,15] are also interesting in the context of novel energy conversion applications; however, demonstra-

tion of their nonthermal nature is particularly challenging at higher pressures in the gas phase [15]. Some authors [17,18] indicate that a secondary thermoelectric effect might dominate the chemicurrent response of some stationary surface processes at high pressures in the gas phase. A reverse argument for the case of H<sub>2</sub> oxidation could be placed forward by recalling that 76% of total energy of the H<sub>2</sub>(g) + 1/2O<sub>2</sub>(g) → H<sub>2</sub>O(g) process on Pt is released during the initial adsorption stages [19], and by observing a nonthermal effect of H<sub>2</sub> adsorption alone in a high pressure environment rather than in vacuum [7–12].

This letter provides clear evidence of participation of nonthermal charge carriers in chemicurrents induced by H<sub>2</sub> adsorption on catalytic sandwich structures of Figure 1 type in 760 Torr N<sub>2</sub>/O<sub>2</sub> mixtures. Here, a continuous Ohmic contact metallization has been fabricated for the entire reverse side of the device. The chemicurrents measured as in Figure 1 diagram, were recorded at room temperature during H<sub>2</sub> adsorption onto the Pt/*n*-SiC/Ag structure preliminary exposed to a N<sub>2</sub>/O<sub>2</sub> mixtures. The thermal effect of the reaction was further imitated for the same sample by exposure to an additional portion of molecular nitrogen, a gas with essentially distinct adsorptive properties [31,32]. The amount and rate of N<sub>2</sub> admission were tuned to produce the same or greater thermal effect on the sample surface as during the process with hydrogen. Both slope and magnitude of the thermal effect were taken into account. In spite of a similar thermal effect of nitrogen admission, a detectable chemicurrent was only induced during the process with hydrogen, and therefore it could not be interpreted as a thermal current.

## 2 Materials and Methods

*Preparation of the Pt/n-SiC structure* for chemicurrent measurements was as follows. Ohmic contact metallization was first fabricated on a non-polished side of a  $0.05 \text{ } \Omega\cdot\text{cm}$   $12\times 16\times 0.33 \text{ mm}$   $n\text{-4H-SiC}$  (0001) substrate by e-beam PVD of 50 nm Ti, 270 nm Cu and 680 nm Ag layers followed by 5 min annealing at  $875^\circ\text{C}$ . A 15 nm cathode layer of 0.9995 Pt of the Figure 1 pattern was deposited next on the opposite polished side of the SiC substrate using standard photolithography and slow-rate PVD techniques. Three 20 mm silver wires of 0.5 mm diameter were also attached with Ag paste to the nanocathode and Ohmic contact terminals. The sample was suspended on these wires in a 4.5 l high vacuum chamber by attaching them to bulk copper contacts of an electrical feedthrough flange. Heating of the sample in vacuum for surface outgassing and electrical properties characterization was performed with two internal 100 W halogen bulbs of controllable intensity. Sample surface temperature was measured with a  $2\times 2\times 0.8 \text{ mm}$  ceramic body RTD sensor, Omega F2020-100-B, positioned in the middle of the nanocathode area. Chemicurrents were recorded with an SRS SIM918 unit connected to a PicoTech ADC-24 data logger.

Reproducibility of the nanofilm resistance and the Pt/SiC Schottky contact I-V dependence was investigated for temperatures from  $26^\circ\text{C}$  to  $240^\circ\text{C}$  to realize structural stability of samples to thermal outgassing cycles and to a thermal effect of adsorption. Resistance of a freshly deposited Pt layer in  $10^{-7}$  Torr vacuum was independent of excitation current in the  $10^{-5}\text{--}10^{-2}$  A range, while it showed a nonlinear dependence on sample temperature. It also slowly drifted down in the entire temperature range as a result of multiple heating cy-

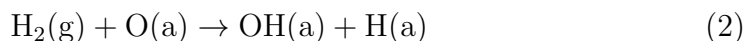
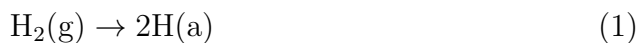
cles. This drift gradually diminished and the resistance-to-temperature curve stabilized and became fully reproducible for the entire 26–240°C range after about 30 hrs annealing at 250°C. The final stable resistance curve is provided on Figure 2 (top), where each data point corresponds to a thermal equilibrium of the sample with the heating setup and the ambient. I-V characteristics of the Pt/SiC contact, shown in Figure 2 (inset) for various sample surface temperatures, were also fully reproducible during the 26–240°C heating cycles. As can be seen, a nonlinear diode-like characteristic is preserved throughout the temperature range. Analysis of the I-V curves gave diode ideality factors of 4–10 and Schottky barrier height in the range 0.60–1.05 eV depending on sample temperature, see Figure 2 bottom plot. A conclusion was then made that the sample is suitable for chemicurrent measurements accompanied by surface thermal outgassing at temperatures up to 140°C, i.e. 100°C below the highest repeatable point in Figure 2 data, for an additional assurance.

*Final surface preparation.* Prior to a first gas admission in all chemicurrent measurement experiments, surface of the sample was outgassed at 140°C for 10 min in  $10^{-7}$  Torr vacuum, followed by 25 min natural cooling to room temperature. A pure synthetic air mixture of 79% N<sub>2</sub> and 21% O<sub>2</sub> at 760 Torr of total pressure was then admitted to the analytical chamber. The resultant adsorption processes led to a 3–4°C increase of surface temperature of the sample; that took another 10 min to reattain thermal equilibrium with the ambient and to complete preparation of sample's surface for chemicurrent measurements.

### 3 Results and Discussion

*Chemicurrent measurements* followed the preparation routine described above under two different *scenarios*: (1) 57 Torr of H<sub>2</sub> gas was admitted to the chamber with the sample at a fast rate of about 110 Torr/s; this resulted in surface temperature and chemicurrent peaks as shown in Figure 3 plots. The surface outgassing procedure was then repeated, and (2) 85 Torr of N<sub>2</sub> gas were admitted at a 130 Torr/s rate. These amount and rate of N<sub>2</sub> admission led a thermal peak with a front slope similar to the one observed during H<sub>2</sub> admission, and with a magnitude even greater than magnitude of the H<sub>2</sub> peak, see Figure 3 (bottom). Figure 3 (top) presents the respective chemicurrent measurements as key results of the present studies. In spite of a greater thermal effect of N<sub>2</sub> admission compared to that of H<sub>2</sub>, admission of nitrogen led to no detectable chemicurrent. Meanwhile, 50–60 nA chemicurrent peaks were repeatedly observed during admission of hydrogen gas. This result did not depend on a particular sequence for the two scenarios to follow one another. Thus, the chemicurrent observed during surface interactions of oxyhydrogen species is due to the underlying charge transfer processes themselves, rather than a thermal effect of these interactions.

Energy required for the hot electron excitation and their subsequent transport over the Schottky barrier, Figure 1, is released on the Pt nanofilm cathode during dissociative hydrogen adsorption events and also interactions of the surface adsorbed (a) oxygen species with molecular hydrogen from the gas phase (g),



Participation of other exoergic stages [19] in the overall  $\text{H}_2(\text{g}) + 1/2\text{O}_2(\text{g}) \rightarrow \text{H}_2\text{O}(\text{g})$  process is also possible. In particular, involvement of the Langmuir-Hinshelwood type reaction  $\text{OH}(\text{a}) + \text{H}(\text{a}) \rightarrow \text{H}_2\text{O}(\text{a})$  could explain the finite width of the chemicurrent peak and its subsequent attenuation to a near zero level, Figure 3, due to saturation of the Pt surface with the  $\text{H}_2\text{O}(\text{a})$  species. Such a saturation is inevitable at room temperatures, because the final product desorption,  $\text{H}_2\text{O}(\text{a}) \rightarrow \text{H}_2\text{O}(\text{g})$ , requires 0.43 eV per water molecule [19].

Magnitudes of the chemicurrent peaks were also investigated as a function of  $\text{O}_2$  fraction in the oxygen-nitrogen mixture prior to hydrogen admission. Statistical averaging over multiple experiments using identical procedures with the same sample gives the data of the Figure 3 upper panel inset plot, where the error bars represent standard deviation of the observed peak magnitudes. Growth of the chemicurrent with the  $\text{O}_2$  fraction tends to diminish for highly oxygen-rich mixtures. Notably, a non-zero current was also detected in pure nitrogen, corresponding to the 0%  $\text{O}_2$  fraction, upon admission of the hydrogen gas. This result can be explained on the basis of the mechanisms (1-2), as the increased oxygen pressure leads to a higher concentration of surface pre-adsorbed oxygen and therefore to a higher rate of the process (1). Meanwhile, in the absence of oxygen molecules in the gas phase, the observed small chemicurrent is driven by the hydrogen dissociative adsorption (2) only.

#### 4 Conclusion

We found that adsorption of molecular hydrogen and nitrogen gases on Pt/SiC planar nanostructure at normal atmospheric conditions leads to generation of a detectable chemicurrent only in the case of hydrogen. Nitrogen admission

conditions were tuned to imitate an equal or greater thermal effect of adsorption as observed during admission of hydrogen gas. Therefore the recorded chemi-current is a result of nonthermal charge transfer processes induced by hydrogen evolution on the catalytic nanostructure. Such a chemi-current can occur not only for surfaces at pre-vacuum conditions, as in the earlier studies [4,5,9], but also for surfaces with prior exposure to a pure nitrogen or synthetic air environment at normal temperature and pressure. The nonthermal chemi-currents can provide novel in-situ techniques for studying mechanisms of heterogeneous catalysis at high gas pressures typical for industrial catalysis, where application of the traditional vacuum based methods, such as LEED, electron energy loss, Auger or ion-scattering spectroscopy is difficult.

This work has been supported by National Science Foundation via grant #1033290.

## References

- [1] B. Mildner, E. Hasselbrink, D. Diesing, Electronic excitations induced by surface reactions of h and d on gold, *Chemical Physics Letters* 432 (1-3) (2006) 133–138.
- [2] D. Diesing, D. Kovacs, K. Stella, C. Heuser, Characterization of atom and ion-induced "internal" electron emission by thin film tunnel junctions, *Nuclear Instruments and Methods in Physics Research B* 269 (11) (2011) 1185–1189.
- [3] E. Hasselbrink, Non-adiabaticity in surface chemical reactions, *Surface Science* 603 (11-12) (2009) 1564–1570.
- [4] E. Karpov, I. Nedrygailov, Solid-state electric generator based on chemically induced internal electron emission in metal-semiconductor heterojunction nanostructures, *Applied Physics Letters* 94 (2009) 214101.
- [5] I. Nedrygailov, E. Karpov, Pd/n-SiC nanofilm sensor for molecular hydrogen detection in oxygen atmosphere, *Sensors and Actuators B* 148 (2) (2010) 388–391.
- [6] E. Karpov, I. Nedrygailov, Nonadiabatic chemical-to-electrical energy conversion in heterojunction nanostructures, *Physical Review B* 81 (20) (2010) 205443.
- [7] B. R. Cuenya, H. Nienhaus, E. McFarland, Chemically induced charge carrier production and transport in pd/sio<sub>2</sub>/n-si(111) metal-oxide-semiconductor schottky diodes, *Physical Review B* 70 (11) (2004) 115322.
- [8] B. Gergen, H. Nienhaus, W. Weinberg, E. McFarland, Chemically induced electronic excitations at metal surfaces, *Science* 294 (2001) 2521–2523.
- [9] H. Nienhaus, Electronic excitations by chemical reactions on metal surfaces, *Surface Science Reports* 45 (1-2) (2002) 3–78.

- [10] H. Nienhaus, H. Bergh, B. Gergen, A. Majumdar, W. Weinberg, E. McFarland, Electron-hole pair creation at ag and cu surfaces by adsorption of atomic hydrogen and deuterium, *Physical Review Letters* 82 (2) (1999) 446–449.
- [11] D. Krix, R. Nuenthel, H. Nienhaus, Generation of hot charge carriers by adsorption of hydrogen and deuterium atoms on a silver surface, *Physical Review B* 75 (7) (2007) 073410.
- [12] U. Hagemann, D. Krix, H. Nienhaus, Electronic excitations generated by the deposition of mg on mg films, *Physical Review Letters* 104 (2) (2010) 028301.
- [13] X. Z. Ji, A. Zuppero, J. Gidwani, G. Somorjai, The catalytic nanodiode: gas phase catalytic reaction generated electron flow using nanoscale platinum titanium oxide schottky diodes, *Nano Letters* 5 (4) (2005) 753–756.
- [14] J. Park, J. Renzas, B. Hsu, G. Somorjai, Interfacial and chemical properties of pt/tio<sub>2</sub>, pd/tio<sub>2</sub>, and pt/gan catalytic nanodiodes influencing hot electron flow, *Journal of Physical Chemistry C* 111 (42) (2007) 15331–15336.
- [15] A. Hervier, J. R. Renzas, J. Y. Park, G. Somorjai, The catalytic nanodiode: gas phase catalytic reaction generated electron flow using nanoscale platinum titanium oxide schottky diodes, *Nano Letters* 9 (11) (2009) 3930–3933.
- [16] J. Trail, M. Graham, D. Bird, M. Persson, S. Holloway, Energy loss of atoms at metal surfaces due to electron-hole pair excitations: First-principles theory of "chemicurrents", *Physical Review Letters* 88 (16) (2002) 166802.
- [17] J. Creighton, M. Coltrin, Origin of reaction-induced current in pt/gan catalytic nanodiodes, *Journal of Physical Chemistry C* 116 (2012) 11391144.
- [18] J. Creighton, M. Coltrin, R. Pawlowski, K. Baucom, Ss-wea1: Characterization of the chemical signal created by co oxidation on pt/gan nanodiodes, in: *AVS 57th International Symposium and Exhibition*, 2010.

- [19] W. Williams, C. Marks, L. Schmidt, Steps in the Reaction  $\text{H}_2 + \text{O}_2 = \text{H}_2\text{O}$  on Pt: OH Desorption at High Temperatures, *Journal of Physical Chemistry* 96 (14) (1992) 5922–5931.
- [20] T. Greber, Charge-transfer induced particle emission in gas surface reactions, *Surface Science Reports* 28 (1997) 1–64.
- [21] E. Hasselbrink, Capturing the complexities of molecule-surface interactions, *Science* 326 (5954) (2009) 809–810.
- [22] A. Wodtke, J. Tully, D. Auerbach, Electronically non-adiabatic interactions of molecules at metal surfaces: Can we trust the born-oppenheimer approximation for surface chemistry?, *International Reviews in Physical Chemistry* 23 (4) (2004) 513–539.
- [23] N. Shenvi, S. Roy, J. C. Tully, Dynamical steering and electronic excitation in no scattering from a gold surface, *Science* 326 (5954) (2009) 829–832.
- [24] G.-J. Kroes, C. Diaza, E. Pijper, R. A. Olsen, D. J. Auerbach, Apparent failure of the born-oppenheimer static surface model for vibrational excitation of molecular hydrogen on copper, *Proceedings of the National Academy of Sciences of the United States of America* 107 (49) (2010) 20881–20886.
- [25] M. Breyse, B. Claudel, L. Faure, H. Latreille, Luminescence during oxygen adsorption on thorium oxide, *Faraday Discussions of the Chemical Society* 58 (58) (1974) 205–214.
- [26] M. Breyse, B. Claudel, M. Guenin, L. Faure, Influence of oxygen traces on the adsorboluminescence given by some gases contacted with thoria, *Chemical Physics Letters* 30 (1) (1975) 149–151.
- [27] A. Bottcher, R. Imbeck, A. Morgante, G. Ertl, Nonadiabatic surface reaction: Mechanism of electron emission in the  $\text{cs} + \text{o}_2$  system, *Physical Review Letters* 65 (16) (1990) 2035–2037.

- [28] M. Cox, J. Foord, R. Lambert, R. Prince, Chemisorptive emission and luminescence: Ii. electron and ion emission from chlorine and bromine reactions with yttrium, titanium, zirconium and hafnium surfaces, *Surface Science* 129 (2-3) (1983) 399–418.
- [29] G. C. Allen, P. M. Tucker, B. E. Hayden, D. F. Klemperer, Early stages in the oxidation of magnesium, aluminium and magnesium/aluminium alloys: I. exoelectron emission and long wavelength photoemission, *Surface Science* 102 (1) (1981) 207–226.
- [30] T. Gesell, E. Arakawa, T. Callcott, Exo-electron emission during oxygen and water chemisorption on fresh magnesium surfaces, *Surface Science* 20 (1) (1970) 174–178.
- [31] M. Wilf, P. Dawson, Adsorption of nitrogen on platinum, *Surface Science* 60 (2) (1976) 561–581.
- [32] E. Miyazaki, I. Kojima, S. Kojima, Chemisorption of molecular nitrogen on palladium surfaces at and above room temperature, *Langmuir* 1 (2) (1985) 264266.

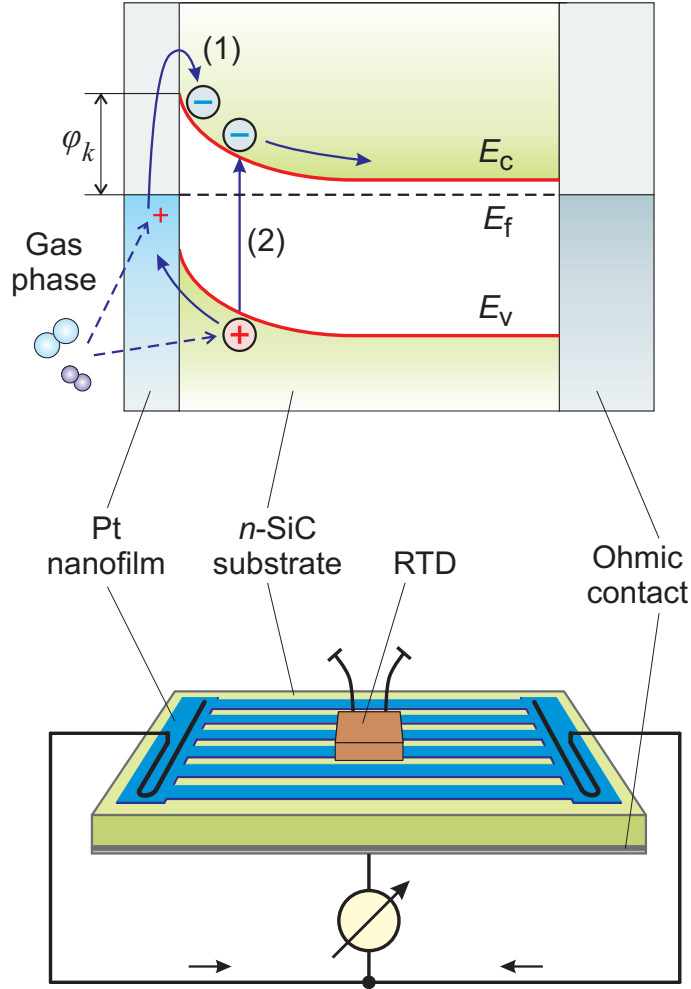


Fig. 1. Top: Possible mechanisms of chemicurrent production at metal nanofilm/semiconductor interfaces; chemically induced generation and subsequent transport of (1) hot electrons and (2) e-h pairs (less probable);  $\varphi_k$  – potential barrier height,  $E_f$  – Fermi level of electrons,  $E_c$  – conduction-band bottom, and  $E_v$  – valence-band top. Bottom: Pt/*n*-SiC device setup discussed here.

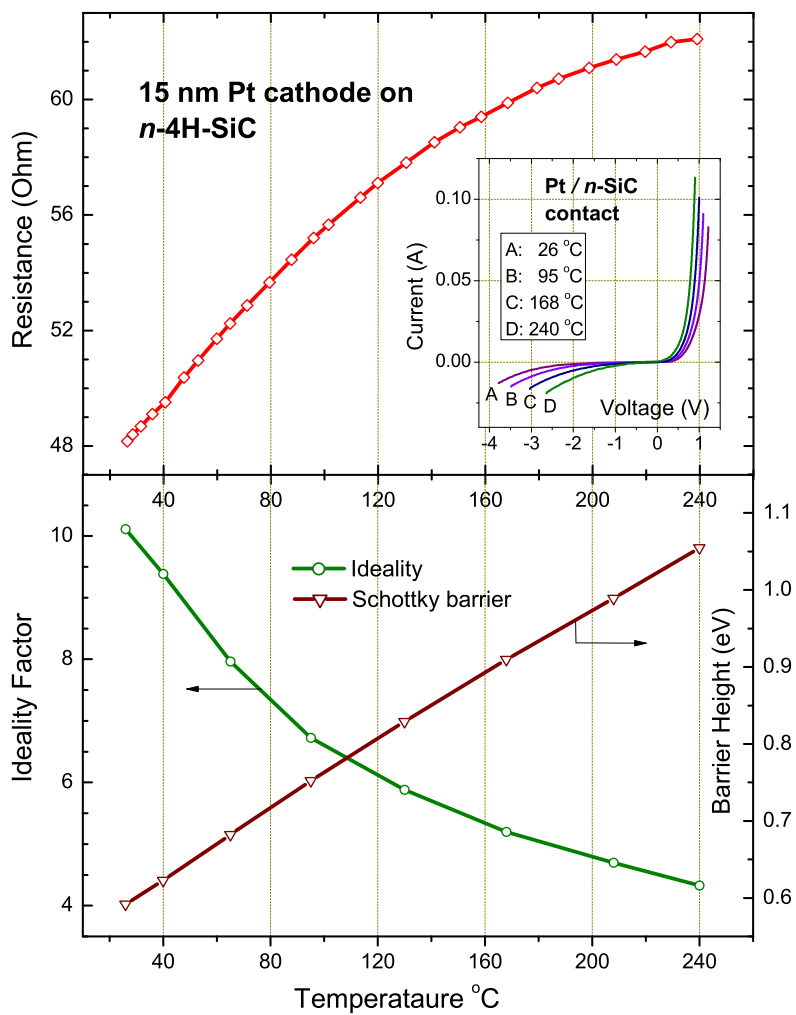


Fig. 2. Electrical properties of Pt/*n*-4H-SiC nanostructure: stable temperature dependence of nanofilm resistance after annealing (top) and diode I-V curves (inset). VAC ideality factor and Schottky barrier height at various temperatures (bottom).

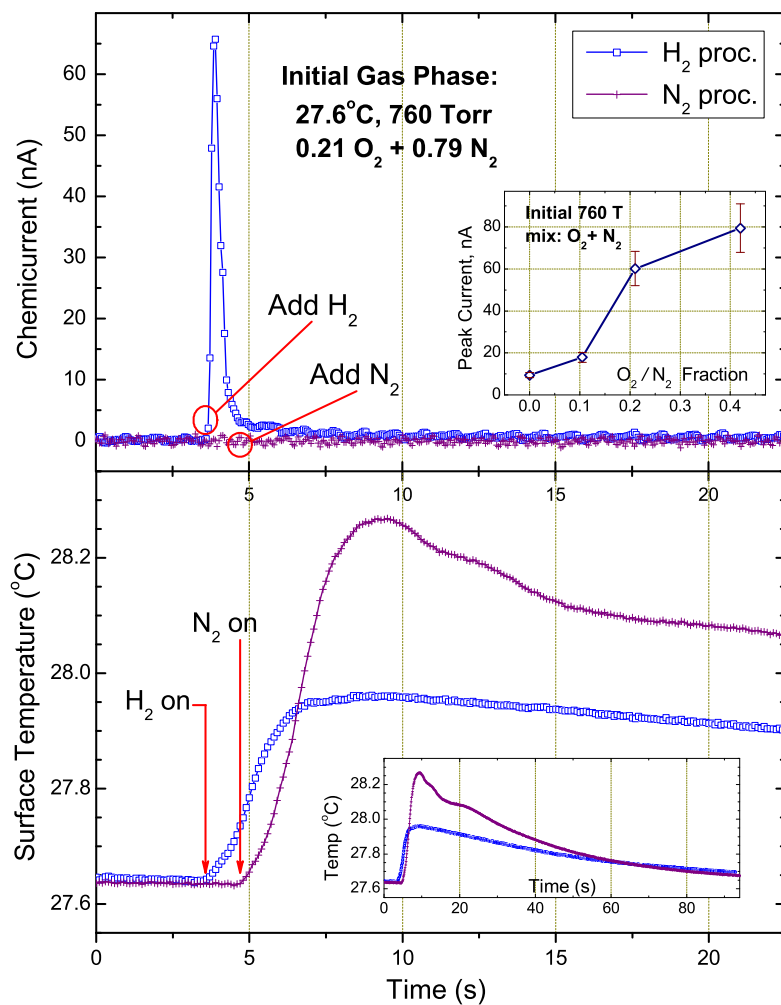


Fig. 3. Kinetics of chemi-current and temperature. Bottom inset plot shows a longer kinetics for the same H<sub>2</sub> and N<sub>2</sub> processes. Inset plot on top shows dependence of the current peak height on ratio of O<sub>2</sub> and N<sub>2</sub> partial pressures in 760 T mixture.